## Vibronic couplings and coherent electron transfer in bridged systems

(Article begins on next page)

09 April 2024

iris - AperTO

# Vibronic Couplings and Coherent Electron Transfer in Bridged Systems

**Raffaele Borrelli,,[b] Amedeo Capobianco,[b] Alessandro Landi,[b] and Andrea Peluso[*b]**

A discrete state approach to the dynamics of coherent electron transfer processes in bridged systems, involving three or more electronic states, is presented. The approach is based on a partition of the Hilbert space of the time independent basis functions in subspaces of increasing dimensionality, which allows for checking the convergence of the time dependent wave function. Vibronic coupling are determined by Duschinsky analysis carried out over the normal modes of the redox partners obtained at high DFT computational level.

## Introduction

Electron transfer reactions are ubiquitous in chemistry and biochemistry. The first mechanistic insights of ET processes were provided by Franck and Libby, who realized that ET rates are regulated by the nuclear motions both of the two molecules which exchange an electron and of the surrounding environment.[1] In analogy with radiative transitions, they asserted that the Franck-Condon principle holds also for thermal ET reactions in solutions, so that ET rates are determined by the overlap between the vibrational states of the initial and final electronic states. The seminal works of Lax and Kubo, and of Marcus, who pioneered the quantitative description of the solvent effects, provided powerful theoretical means for computing Franck-Condon factors, posing the fundamentals for modeling ET reactions in condensed phases.[2–5] Apart from

vibrational contributions, the second crucial factor which control ET rates is the electronic coupling term. Works on systems in which the two redox centers are rigidly spaced by an ET inert bridge, i.e. a system whose unoccupied electronic levels are too high in energy for being accessible to a transferring electron, made it rapidly clear that the electronic coupling term must involve not only the direct interactions between the electronic clouds of the two redox partner but also their offresonance couplings with the virtual electronic states of the bridging system.[6–8] That bridged mediated ET mechanism, analogue to resonance Raman scattering in radiative transitions and to magnetic interactions in solids, was called superexchange mechanism.

Since bridged systems are of outstanding importance in biochemistry, ET via superexchange has been the subject of several theoretical works; coherent quantum dynamics as well as dissipative models have been developed in the past to explore ET dynamics in three-electronic states system.[9–22] Herein we report a theoretical approach based on numerical solution of

[b] *Department of Chemistry and Biology, University of Salerno, I-10125 Fisciano (SA), Italy E-mail: apeluso@unisa.it*
[a] *Department of Agricultural, Forestry and Food Science, University of Torino, Via Leonardo da Vinci 44, I-10095 Grugliasco, Italy;*

the time dependent Schrödinger equations for systems characterized by three or more electronic states, each of them modeled in the harmonic approximation using parameters obtained by highly reliable density functional theory (DFT) computations. Combining the results of DFT or *ab-initio* computations with quantum dynamics simulations of ET rates is still a challenging task,[23–28] which hopefully can lead to a deeper understanding of the mechanisms of ET reaction occurring in biochemical systems as well as in nanoelectronic devices. Here we will apply the formalism to coherent hole transfer processes in DNA, mimicking hole transfer between two guanines separated by one or more adenine and thymine units.

# 1 The Hamiltonian matrix

Let us consider a supramolecular system characterized by $L$ weakly interacting molecular sites in which a charge, an electron or a hole, has been injected. In such a supramolecular assembly each molecular unit, $i$, can be found either in its neutral, $|i_N\rangle$, or charged state, $|i_C\rangle$, giving rise to $L$ low lying diabatic electronic states, each of them corresponding to the additional electron or hole fully localized on one molecular site. Let $|l\rangle$ denote the electronic state in which the charge is localized on the $l$-th site; because the electronic coupling is weak, $|l\rangle$ can be well represented by the direct product of the eigenstates of the non-interacting molecular units:

$$|l\rangle = |l_C\rangle \prod_{i \neq l}^{L} |i_N\rangle \qquad (1)$$

with:

$$H_{iX}^{(el)}|i_X\rangle = U_{iX}(\mathbf{Q}_{iX})|i_X\rangle, \qquad X = C,N \qquad i = 1,2...L. \qquad (2)$$

where $H_{iX}^{(el)}$ is the electronic Hamiltonian operator of the isolated $i$-th molecular unit in its redox state $X = C/N$, $U_{iX}(\mathbf{Q}_{iX})$ is the electronic energy of the isolated $i$-th molecular unit, and $\mathbf{Q}_{iX}$ its normal modes of vibration.

Throughout this paper we will adopt harmonic approximation for the $U_{iX}$'s:

$$U_{iX} = E_{iX}^0 + \frac{1}{2}\mathbf{Q}_{iX}^\dagger \omega_{iX}^2 \mathbf{Q}_{iX} \qquad (3)$$

where $\omega_{iX}$ is the diagonal matrix of the vibrational frequencies of the normal modes of the $i$-th unit in its $X$ electronic state ($X = C,N$).

The Hamiltonian operator of the whole $L$-site system can then be written:[13]

$$\mathscr{H} = \sum_{l,m}^{L} |l\rangle \mathscr{H}_{lm} \langle m|, \qquad (4)$$

with:

$$\mathscr{H}_{lm} = \langle l | \mathscr{T}_N + \mathscr{H}_{el} | m \rangle. \qquad (5)$$

where $\mathscr{T}_N$ and $\mathscr{H}_{el}$ include all the nuclear and electronic coordinates of the whole molecular assembly.

The total time-dependent wavefunction is expanded over a set of Born-Oppenheimer product wavefunctions:

$$\Psi(t) = \sum_{l,\bar{v}_l} \mathbf{C}_{\bar{v}_l}^{(l)}(t) |l, \bar{v}_l\rangle. \qquad (6)$$

in which the vibrational basis functions $|\bar{v}_l\rangle$ for the $l$-th electronic state are given by the direct product of the vibrational states of each molecular unit and the expansion coefficients are determined by solving the time-dependent Schrödinger equation:

$$-i\hbar \begin{pmatrix} \dot{\mathbf{C}}_{\bar{v}_1}^{(1)} \\ . \\ . \\ \dot{\mathbf{C}}_{\bar{v}_L}^{(L)} \end{pmatrix} = \begin{pmatrix} \mathbf{H}_{11} & \mathbf{H}_{12} & . & . & \mathbf{H}_{1L} \\ & . & . & . & \\ & . & . & . & \\ \mathbf{H}_{1L}^\dagger & \mathbf{H}_{2L}^\dagger & . & . & \mathbf{H}_{LL} \end{pmatrix} \begin{pmatrix} \mathbf{C}_{\bar{v}_1}^{(1)} \\ . \\ . \\ \mathbf{C}_{\bar{v}_L}^{(L)} \end{pmatrix}, \qquad (7)$$

with initial conditions specifying the initial state of the system. Each $\mathbf{H}_{lm}$ in equation 7 is a matrix whose size depends on the sizes of the vibrational basis sets chosen for each electronic states $l$ and $m$.

The computation of the diagonal blocks of the Hamiltonian matrix, is straightforward; indeed the $\mathbf{H}_{ll}$ are diagonal matrices, whose elements are simply given by the eigen-energies of multidimensional harmonic oscillators. By denoting with $n_{i,lk}^{(\alpha)}$ the vibrational quantum number of the $\alpha$-th normal mode of the $i$-th molecular unit in the $lk$-th vibronic state, the diagonal elements take the form:

$$H_{lk,lk} = \sum_{i=1}^{L}\left[ \sum_{\alpha} \hbar n_{i,lk}^{(\alpha)} \omega_{i,l}^{(\alpha)} \right] + E_l, \qquad (8)$$

where $E_l$ is the electronic energy of the $l$-th electronic state; the index $i$ runs over all the molecular units and $\alpha$ over the normal modes of the $i$-th unit. The zero point energy does not appear in the eq 8 because its contribution can be conveniently included in the electronic energy term.

After integration over the electronic coordinates, neglecting the weak dependence of the electronic couplings on the nuclear coordinates, the coupling terms between the vibronic states of $|l\rangle$ and $|m\rangle$ are given by:

$$H_{l\bar{v}_l, m\bar{v}_m} = H_{lm} \cdot \left\langle \bar{v}_{ml} | \bar{v}_{mm} \right\rangle \left\langle \bar{v}_{ll} | \bar{v}_{lm} \right\rangle \cdot \prod_{i \neq l,m} \delta_{\bar{v}_{il}, \bar{v}_{im}}, \qquad (9)$$

where $H_{lm} = \langle l | \mathscr{H}^{el} | m \rangle$ is the electronic coupling term, and $\left\langle \bar{v}_{ml} | \bar{v}_{mm} \right\rangle$ and $\left\langle \bar{v}_{ll} | \bar{v}_{lm} \right\rangle$ are the multidimensional Franck-Condon integrals over the normal modes of the two molecular units involved in the $l \to m$ non-radiative transition.

The basic ingredients to build up the Hamiltonian matrix which determines the time evolution of the system are therefore: *i*) the relative energy of the $L$ vibronic ground states (including the zero point contribution); *ii*) the normal modes of each electronic states, which according to the above assumptions can be evaluated separately for each molecular component, *c.f.* eq 2; *iii*) the electronic coupling term $H_{lm}$ and *iv*) the Franck-Condon integrals.

In any discrete state approach to quantum dynamics, the selection of the vibrational states to be used in the time evolution is probably the most important problem to deal with. Different strategies to reduce the size of the vibronic basis set have been proposed in the literature.[29] The approach we will use here is based on the idea of partitioning the entire Hilbert space in a set of subspaces which differ in the number of vibrations which are allowed to be simultaneously excited. Thus the entire Hilbert space H spanned by the Hamiltonian of eq. 7 can be partitioned as

$$H = \bigcup_c S_c$$

where $S_c$ is the space spanned by the states in which only $c$ vibrations are simultaneously excited, with a given maximum quantum number for each of them. Using such a partition the wavefunction of eq. 6 can be more specifically written as:

$$\Psi(t) = \sum_{l}^{L}\left[ \sum_{c=1}^{N} \sum_{i_1 \dots i_C}^{\binom{N}{c}} \sum_{v_{i_1} \dots v_{i_c}} C_{v_{i_1} \dots v_{i_c}}(t) | v_{i_1} \dots v_{i_c} \rangle \right] | l \rangle =$$

$$\sum_{l}\left[ C_0^{(l)}(t)|0\rangle + \sum_i \sum_{v_i} C_{v_i}^{(l)}(t)|v_i\rangle + \sum_{ij}^{\binom{N}{2}} \sum_{v_i v_j} C_{v_i v_j}^{(l)}(t)|v_i v_j\rangle + \dots \right] | l \rangle$$
$$(10)$$

where for sake of simplicity we have dropped the index $l$ in the vibrational basis set.

This partition of the Hilbert space stems from the observation that in molecular systems the larger the number of excited modes the smaller the Franck-Condon integrals associated to a specific electronic transitions. In the field of molecular spectroscopy this approach has been exploited by Santoro *et al.* and formalised by Janckowiack *et al.*.[30,31] Since in our methodology the coupling between two vibronic states is directly proportional to the corresponding FC integrals, it is expected that the effect of states with a significant number of excited vibrations on the overall dynamics. will only be marginal. This heuristic approach allows to significantly restrict the active space of the problem and the associated numerical complexity still retaining the most important features of the dynamical behaviour of the system.

As concerns the choice of the active vibrational modes, *i.e.* modes which are allowed to change their quantum number during the transition, they can be determined by the affine Duschinsky's transformation: [32]

$$\mathbf{Q}_l = \mathbf{J}\mathbf{Q}_m + \mathbf{K}, \qquad (11)$$

where $\mathbf{Q}_l$ and $\mathbf{Q}_m$ are the normal mode vectors of $|l\rangle$ and $|m\rangle$, $\mathbf{J}$ is the rotation matrix and $\mathbf{K}$ the displacement vector.

The rotation matrix $\mathbf{J}$ and the displacement vector $\mathbf{K}$ can be easily determined once the equilibrium geometries and the normal modes of the two electronic states are known. [33–38].

In order to further reduce the overall computational costs, the computation of the FC integrals has been carried out by using the separate-mode approximation, which allows factorization of the multidimensional FC integrals into the product of one-dimensional integrals. [39] It is an approximate method for fast FC computations, which corresponds roughly to neglecting the off diagonal terms of the Duschinsky transformation but taking into account the changes of the vibrational frequencies of the vibrational modes.

## 2 Coherent hole transfer in DNA

Long distance hole transfer (HT) in DNA is of outstanding importance; the chemico-physical properties of DNA under oxidative stress, [40]? as well as the possibility of using DNA in molecular electronics and molecular computing, [41–45] depend on the efficiency with which an electron hole can move along a strand. Steady state photocleavage analyses and time resolved spectroscopical methods have shown that HT can cover distances up to 200 Å before irreversible oxidation takes place. [46–60] Oxidation preeminently occur at guanine (G), the nucleobase with the lowest oxidation potential, [61–65] particularly at sites comprising sequences of multiple GC base pairs, [66–73] but oxidative damages at adenine

(A) and thymine (T) have also been found, [74,75] showing that HT in DNA is a very complex phenomenon, in which several chemico-physical factors play a role.

Time resolved spectroscopy and steady state oxidative damage analyses point toward an incoherent multistep hopping mechanism, [49,60,76–82] in which the hole migrates essentially by hopping between G neighboring sites, [59] with the possibility of tunnelling over short distances, when two G sites are separated by two or almost three A and/or T sites. The hopping process is in most of the cases slow, thus limiting potential applications to nano-scale electronic devices, [83,84] but since significant enhancements of HT rates have been observed both by including in the strand modified nucleobases, with a lower oxidation potentials than natural ones, or by using sequences consisting of blocks of homopurine sequences, [85,86] research in the field is still very active. [83,84,87–90]

Many theoretical studies at very high level of sophistication have been performed in the past concerning the mechanism of HT in DNA. [76,79,87,91–99] Herein, we focus on coherent ET process taking place between two G separated by up to three A or T units, a problem which has been experimentally addressed by Giese, who measured the ratios of the oxidative damages occurring at two G:C steps, as a function of the interposed A:T steps. [100] Our numerical simulation of HT in short DNA tracts starts from the analysis of the equilibrium position displacements upon oxidation of the redox half-pairs $G/G^+$, $A/A^+$, $T/T^+$. The components of the $\mathbf{K}$ vectors, c.f. Eq, 11, which are by far the quantities which play a major role in determining the value of the effective couplings between vibronic states, are reported in Tab. 1 for the three redox half-pair $G/G^+$, $A/A^+$, and $T/T^+$, together with their contribution to the total reorganization energy, evaluated by using harmonic approximation. Planarization of the exocyclic amino group is the most important geometrical change caused by oxidation of A and G nucleobases. [101] In the case of neutral G, the computed values

of the out-of-plane bending of the two exocyclic amino hydrogens is 27.8 degrees whereas in the oxidized form the amino group is almost planar. For $A^+$ the exocyclic amino group is also planar, whereas in the neutral form the out-of-plane bending is 13.2 degrees. The predominat role played by the planarization of the amino group is confirmed by MP2 computations of the optimum geometries of neutral and oxidized nucleobases, which yield a slightly higher degree of distortion than DFT; more details about geometry change for the pairs $A/A^+$ and $G/G^+$ can be found in ref[99]. As concerns $T/T^+$ redox half-pair, the most significant geometrical changes upon oxidation concern C-C and C-N ring bonds and ring valence bending coordinates; the displacements are small, see tab. 2, notwithstanding the computed B3LYP reorganization energy amounts to 1935 cm$^{-1}$, comparable to those of the other two nucleobases: 1622 and 2294 cm$^{-1}$ for A and G, respectively. Inspection of tab. 2 show that more than 80% of the reorganization energy arises from a subset of 13, 8 and 5 normal modes of G, A, and T, respectively. Thus a model including only those modes should provide a qualitatively correct picture of the HT dynamics.[102,103] Furthermore, due to the high frequency of the most displaced vibrations with respect to the thermal quantum at room temperature, we can neglect any temperature effect and assume that the system is initially in its vibrational ground state.

Before considering HT in bridged systems we have first studied the hole-hopping in the pair $GA^+$ with the aim of checking the convergence properties of the proposed methodology. The 21 degrees of freedom of tab. 2 have been used in computations; the energy difference between the initial and final diabatic states have been set to 0.4 eV from the observed oxidation potentials, whereas $V_{AG}$ has been set to 0.1 eV, an average value taken from the results of voltammetric measurements and DFT computations,[88–90] see below for further details.

The results are reported in Fig. **??**, where the population decay of the initial state, corresponding to the hole completely localized on the A moiety, are reported as a function of time for different choices of the Hilbert subspaces, defined in Eq. 10. When the vibrational basis set included states with at most three vibrations simultaneously excited the results provide a qualitatively good description of the process. Adding the states with four simultaneously excited vibrations provides an almost converged result, since at higher excitation level the population decay of the initial state does not show any significant variation. The transition time for such ultrafast ET process is about 20 fs, very similar to that predicted by using the Fermi Golden Rule, dashed blach line in Fig. **??**, using the density of states evaluated at 298 K including the whole set of normal modes of both redox partners.[27,99,104].

The results of fig. **??** demonstrate that the proposed methodology has good scaling properties, indeed we have obtained a converged dynamics by using only 1.5 10$^5$ basis function. A complete tensor product basis set would have required a number of the order of magnitude on 10$^9$, *i.e.* comprised between 21$^7$ and 21$^{10}$. The favourable scaling properties of the methodology obviously lead to an increased algorithmic complexity, mainly due to the necessity of computing the proper FC integrals on-the-fly during the dynamics.

We have then considered hole dynamics for GAG and GTG triads, GAAG, GAGG, and GTTG tetrads, and GAAAG, GAAGG, GTTGG, and GTTTG pentads.

The parameters used in dynamics are the following: $E_G = 0$, $E_A = 0.4$, $E_T = 0.5$, $V_{AA}=0.3$, $V_{AG} = V_{GG} = 0.1$, and $V_{TT} = 0.08$ eV.

The energy differences between diabatic states have been taken from oxidation potentials of nucleobases in solution,[61–64] whereas electronic couplings have been estimated as the best parameters to reproduce within the limit of a simple tight binding approximation the results of voltammetric

**Table 1** Frequencies ($\omega$, cm$^{-1}$), intramolecular reorganization energies ($E_r$, cm$^{-1}$), and equilibrium position displacements (**K**, Å uma$^{-1/2}$) of the most displaced normal modes of G/G$^+$, A/A$^+$, and T/T$^+$ redox pairs.

| G/G$^+$ | | | A$^+$/A | | | T$^+$/T | | |
|---|---|---|---|---|---|---|---|---|
| $\omega$ | $E_r$ | **K** | $\omega$ | $E_G$ | **K** | $\omega$ | $E_r$ | **K** |
| 338 | 76 | -0.211 | 724 | 88 | -0.106 | 387 | 88 | 0.00 |
| 435 | 223 | -0.282 | 1328 | 83 | 5.62E-002 | 549 | 132 | 0.112 |
| 477 | 80 | 0.154 | 1143 | 83 | -6.55E-002 | 739 | 74 | 0.112 |
| 521 | 166 | -0.203 | 1353 | 204 | 8.66E-002 | 1375 | 289 | -0.132 |
| 528 | 78 | -0.137 | 1367 | 84 | -5.52E-002 | 1425 | 233 | 0.00 |
| 1230 | 75 | -5.79E-002 | 1510 | 424 | 0.112 | 1503 | 155 | -1.9E-002 |
| 1366 | 85 | -5.53E-002 | 1622 | 109 | 5.29E-002 | 1688 | 732 | -0.134 |
| 1403 | 121 | 6.42E-002 | 1639 | 167 | -6.47E-002 | 1735 | 187 | -3.7E-002 |
| 1435 | 90 | -5.43E-002 | | | | | | |
| 1477 | 259 | 8.95E-002 | | | | | | |
| 1526 | 80 | 4.82E-002 | | | | | | |
| 1639 | 488 | -0.111 | | | | | | |
| 1742 | 160 | -5.96E-002 | | | | | | |
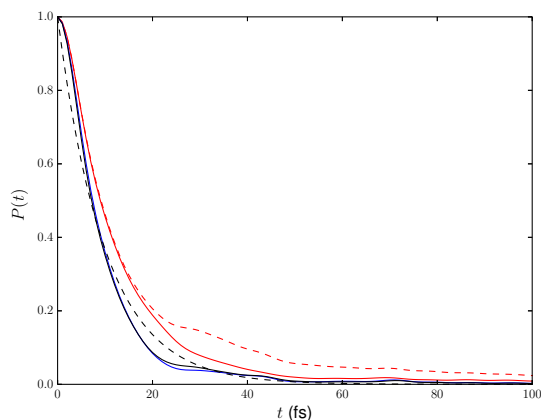
**Fig. 1** Population decay of the $A^+G$ tract computed using different Hilbert subspaces: $N(A^+G)=1$, $N(AG^+)=3$ dashed red line; $N(A^+G)=2$, $N(AG^+)=3$ red line; $N(A^+G)=1$, $N(AG^+)=4$ blue line; $N(A^+G)=1$, $N(AG^+)=5$ black line. The exponential decay predicted by the Fermi Golden Rule, dashed black line, is also reported for comparison.

measurements of A and G rich oligonucleotides,[89,90,105] without considering vibrational overlap effects, so that they should be considered as a lower limit estimates.

The results of all dynamics simulations are collected in Tab. **??**. We started by completely neglecting vibrational effects; that approximation leads to a very facile HT by tunnelling: for GAG, GAAG, and GTG, HT between the two ending Gs occurs on subpicosecond timescales, whereas for GAAAG, GTTG, and GTTTG transition times are significantly longer. Particularly intriguing is the case of GAAAG, where the comparatively longer transition time is due to the establishment of a delocalized domain, comprising all the five nucleobases; only in that case the electronic states of the brige are populated in dynamics. The establishment of delocalized domains in DNA is a very important issue, we will be back later on that important point.

Inclusion of vibrational effects at the lowest level of approx-imation, i.e. considering only the vibronic ground state of each electronic state, has a strong effect on the computed transition times, which increase of more than one order of magnitude in the case of A bridging units and even more for T ones. Noteworthy coeherence effects are loss in the case of GTTTG, where HT transition time is longer than 1 ns.

Increasing the dimension of the Hilbert subspaces used in dynamics lead as expected to shorter transition times. The effect is comparatively smaller in the case of A bridges, because of the significantly higher electronic coupling term between consecutive As. In the case of GAG, we have obtained convergent transition times using double excitation on the A bridge ($N_A=2$). At this exploratory stage, we have used used the smallest Hilbert subspaces for G units ($N_G=1$), inasmuch in coherent superexchange mechanism the excited states of the bridge are expected to play the major role.

The time evolutions of the populations of the initial states, corresponding to a hole fully localized on a single G, together with those of the bridge states (summed over all vibronic states of the bridge) for GAG and GAAG are reported in Fig. 2. The model Hamiltonians for GAG and GAAG include all the modes reported in tab. 2, i.e. 34 and 42 vibrational degrees of freedom for GAG and GAAG, respectively. The population of the initial state in which the charge is initially fully localized on a guanine site halves in about 200 fs for GAG and slightly longer for GAAG; the transfer mechanism is clearly a coherent superexchange, inasmuch the bridge states exhibit negligible populations at all the times, see dashed lines in Fig. 2.

As concerns HT trough thymine bridges, tunnelling is predicted to be quite efficient in GTG and GTTG tracts, provided that a sufficient number of vibronic states are considered in dynamics, whereas for GTTTG tunnelling occurs on nanosecond timescale, which, apart from problem concerning coherence on such long time intervals, is more or less comparable with the transition times predicted for the hopping mechanism.[99]

**Table 2** Transition times ($\tau$, ps) at different level of approximation for HT between the ending Gs in GAG, GAAG, GAAAG, GTG, GTTG, and GTTTG.

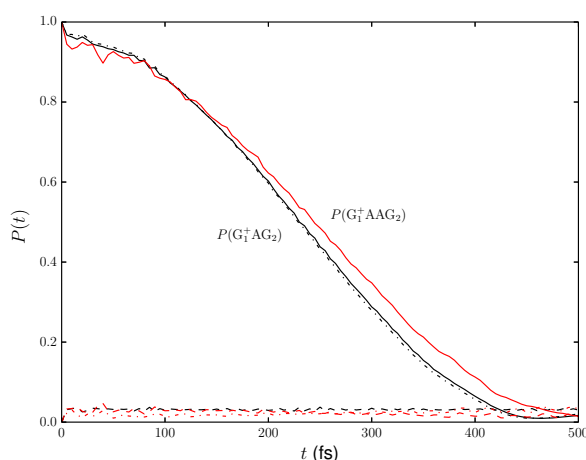| $N_i$ | $N_b$ | $N_f$ | GAG | GAAG | GAAAG | GTG | GTTG | GTTTG |
|-------|-------|-------|------|------|-------|------|------|-------|
| | no FC | | 0.042 | 0.021 | 0.68 | 0.066 | 0.47 | 3.0 |
| 0 | 0 | 0 | 0.67 | 4.6 | 31.0 | 5.6 | 267.0 | > 1000 |
| 1 | 1 | 1 | 0.52 | 0.68 | 0.72 | 0.88 | 12 | 152 |
| 1 | 2 | 1 | 0.46 | 0.48 | 0.36 | 0.64 | 6 | |
| 1 | 3 | 1 | 0.46 | | | 0.62 | | |



**Fig. 2** Hole-transfer dynamics in $G^+AG$ (black) and GAAG (red) tracts. Full lines refer to population decay of the initial state, dashed lines to the total population of the bridge vibronic states.

Giese has shown that hole transfer between guanines in duplexes can take place both by a coherent superexchange mechanism and by a thermally induced hopping process; the efficiency of the tunnelling mechanism decreases rapidly as the number of the bridging T:A steps increases, the bridge influence vanishes completely for three or more intervening T:A steps. Those results were attributed to a shift in the HT mechanism from coherent superexchange at short distances to thermally induced hopping at long distances.[100] Our results are in substantial good agreement with those experimental findings for bridges consisting of thymine tracts. Noteworthy, in Giese's experiment intrastrand HT involve T homo-bases tracts, whereas of course A tracts would be involved in interstrand HT. As concerns intrastrand HT along A tracts, our results predict that HT efficiency does not significantly depend on the number of intervening As, up to three consecutive As. We attribute that peculiar behavior

There is indeed growing experimental and theoretical evidence that sequences consisting of two or more consecutive homobases can form delocalized domains, in which the hole is stabilized by resonance,[50,60,66–73,88–90,106–109] but the question about their real establishment is still under vivid debate

## 3 Computational details

Equilibrium geometries, normal modes, and vibrational frequencies of G and A in their neutral and cationic form were obtained at DFT level using the standard B3LYP functional with the 6-311++G(d,p) basis set. Solvent (water) effects have been estimated by using the polarizable continuum model (PCM);[110] the G09 package have been used for all electronic wavefunction computations.[111] Franck-Condon integrals and the density of states used in the evaluation of the Fermi Golden Rule rate constant have been computed by using a development version of the MolFC package,[37,112] Full details about

implementation of the generating function approach can be found in ref.s [27,104,113,114]. In all FC calculations, the curvilinear coordinate representation of the normal modes has been adopted to prevent that a large displacement of an angular coordinate could reflect into large shifts of the equilibrium positions of the involved bond distances. That is unavoidable in rectilinear Cartesian coordinates and requires the use of high order anharmonic potentials for its correction. [38,113,115–118]

The numerical solution of the time-dependent Schödinger equation has been carried out with an orthogonalised Krylov subspace method. [29,119]

# Acknowledgement

# References

1  W. F. Libby, *J. Phys. Chem.*, 1952, **56**, 863âĂŞ–868.

2  M. Lax, *J. Chem. Phys.*, 1952, **20**, 1752.

3  R. Kubo and Y. Toyozawa, *Prog. Theor. Phys.*, 1955, **13**, 160.

4  R. A. Marcus, *J. Chem. Phys.*, 1956, **24**, 966–978.

5  R. A. Marcus, *J. Chem. Phys.*, 1956, **24**, 979–989.

6  M. George and J. S. Griffith, *The enzymes I*, Elsevier Academic Press, New York, 1959.

7  J. Halpern and L. Orgel, *Discuss. Faraday Soc.*, 1960, **29**, 32.

8  H. M. McConnell, *J. Chem. Phys.*, 1961, **35**, 5008.

9  J. S. Joseph and W. Bialek, *J. Phys. Chem.*, 1993, **95**, 3245–âĂŞ3256.

10  M. D. Todd, A. Nitzan and M. A. Ratner, *J. Phys. Chem.*, 1993, **97**, 29âĂŞ–33.

11  R. Egger, C. H. Mak and U. Weiss, *J. Chem. Phys.*, 1994, **100**, 2651–2660.

12  R. Egger and C. H. Mak, *J. Phys. Chem.*, 1994, **98**, 9903–9918.

13  M. Bixon and J. Jortner, *Adv. Chem. Phys.*, 1999, **106**, 35–203.

14  Y. Hu and S. Mukamel, *Chem. Phys. Lett.*, 1989, **160**, 410.

15  J. Tang, Z. Wang and J. R. Norris, *J. Chem. Phys.*, 1993, **99**, 979–984.

16  O. Kühn, V. Rupasov and S. Mukamel, *J. Chem. Phys.*, 1996, **104**, 5821–5833.

17  S. S. Skourtis and S. Mukamel, *Chem. Phys.*, 1995, **197**, 367–388.

18  S. H. Lin, *J. Chem. Phys.*, 1989, **90**, 7103–7113.

19  H. Sumi and R. A. Marcus, *Chem. Phys. Lett.*, 1996, **252**, 85–91.

20  A. A. Stuchebrukhov, *J. Chem. Phys.*, 1996, **105**, 10819.

21  H. Sumi and T. Kakitani, *J. Phys. Chem. B*, 2001, **105**, 9603–9622.

22  X. Chu and Y. Zhao, *J. Theor. Comput. Chem.*, 2009, **8**, 1295–1307.

23  A. Warshel, *Acc. Chem. Res.*, 1981, **14**, 284.

24  A. Warshel, Z. Chu and W. Parson, *Science*, 1989, **246**, 112–116.

25  A. Warshel and W. W. Parson, *Ann. Rev. Phys. Chem.*, 1991, **42**, 279.

26  A. Warshel and W. W. Parson, *Q. Rev. Biophys.*, 2001, **34**, 563–679.

27  R. Borrelli and A. Peluso, *Phys. Chem. Chem. Phys.*, 2011, **13**, 4420.

28  A. Peluso, *Curr. Org. Chem.*, 2010, **14**, 90.

29  C. Lubich, *From Quantum to Classical Molecular Dynamics: Reduced Models and Numerical Analysis*, European Mathematical Society Publishing House, Zuerich, Switzerland, 2008.

30  F. Santoro, A. Lami, R. Improta, J. Bloino and V. Barone, *J. Chem. Phys.*, 2008, **128**, 224311.

31  H.-C. Jankowiak, J. L. Stuber and R. Berger, *J. Chem. Phys.*, 2007, **127**, 234101.

32  F. Duschinsky, *Acta Phisicochim. URSS*, 1937, **7**, 551.

33  T. E. Sharp and K. M. Rosenstock, *J. Chem. Phys.*, 1964, **41**, 3453.

34  A. Warshel and M. Karplus, *Chem. Phys. Lett.*, 1972, **17**, 7.

35  A. Peluso, F. Santoro and G. Del Re, *Int. J. Quant. Chem.*, 1997, **63**, 233.

36  J. R. Reimers, *J. Chem. Phys.*, 2001, **115**, 9103.

37  R. Borrelli and A. Peluso, *J. Chem. Phys.*, 2003, **119**, 8437.

38  R. Borrelli and A. Peluso, *J. Chem. Phys.*, 2006, **125**, 194308.

39  R. Borrelli and A. Peluso, *J. Chem. Phys.*, 2008, **128**, 044303.

40  Y. Rokhlenko, J. Cadet, N. E. Geacintov and V. Shafirovich, *J. Am. Chem. Soc.*, 2014, **136**, 5956–5962.

41  E. Braun, Y. Eichen, U. Sivan and G. Ben-Yoseph, *Nature*, 1998, **391**, 775–778.

42  D. Porath, A. Bezryadin, S. de Vries and C. Dekker, *Nature*, 2000, **403**, 635–638.

43 J.-J. Shu, Q.-W. Wang and K.-Y. Yong, *Phys. Rev. Lett.*, 2011, **106**, 188702.

44 K.-H. Yoo, D. H. Ha, J.-O. Lee, J. W. Park, J. Kim, J. J. Kim, H.-Y. Lee, T. Kawai and H. Y. Choi, *Phys. Rev. Lett.*, 2001, **87**, 198102.

45 R. G. Endres, D. L. Cox and R. R. P. Singh, *Rev. Mod. Phys.*, 2004, **76**, 195–214.

46 C. J. Murphy, M. R. Arkin, Y. Jenkins, N. D. Ghatlia, S. H. Bossmann, N. J. Turro and J. K. Barton, *Science*, 1993, **262**, 1025–1029.

47 C. J. Murphy, M. R. Arkin, N. D. Ghatlia, S. H. Bossmann, N. J. Turro and J. K. Barton, *Proc. Natl. Acad. Sci. USA*, 1994, **91**, 5315–5319.

48 G. B. Schuster, *Acc. Chem. Res.*, 2000, **33**, 253–260.

49 B. Giese, *Acc. Chem. Res.*, 2000, **33**, 631–636.

50 B. Giese and S. Wessely, *Angew. Chem. Int. Ed.*, 2000, **39**, 3490–3494.

51 C. Wan, T. Fiebig, O. Schiemann, J. K. Barton and A. H. Zewail, *Proc. Natl. Acad. Sci. USA*, 2000, **97**, 14052–14055.

52 F. D. Lewis, X. Liu, S. Miller, R. T. Hayes and M. R. Wasielewski, *Nature*, 2000, **406**, 51–53.

53 F. D. Lewis, R. L. Letsinger and M. R. Wasielewski, *Acc. Chem. Res.*, 2001, **34**, 159–170.

54 S. Hess, M. Götz, W. B. Davis and M. E. Michel-Beyerle, *J. Am. Chem. Soc.*, 2001, **123**, 10046–10055.

55 F. D. Lewis, X. Liu, S. Miller, R. T. Hayes and M. R. Wasielewski, *J. Am. Chem. Soc.*, 2002, **124**, 4568–4569.

56 F. D. Lewis, J. Liu, X. Zuo, R. T. Hayes and M. R. Wasielewski, *J. Am. Chem. Soc.*, 2003, **125**, 4850–4861.

57 T. Takada, K. Kawai, S. Tojo and T. Majima, *J. Phys. Chem. B*, 2003, **107**, 14052–14057.

58 T. Takada, K. Kawai, M. Fujitsuka and T. Majima, *Proc. Natl. Acad. Sci. USA*, 2004, **101**, 14002–14006.

59 S. Kanvah, J. Joseph, G. B. Schuster, R. N. Barnett, C. L. Cleveland and U. Landman, *Acc. Chem. Res.*, 2009, **43**, 280–287.

60 J. C. Genereux and J. K. Barton, *Chem. Rev.*, 2010, **110**, 1642–1662.

61 M. Faraggi, F. Broitman, J. B. Trent and M. H. Klapper, *J. Phys. Chem.*, 1996, **100**, 14751–14761.

62 T. Caruso, M. Carotenuto, E. Vasca and A. Peluso, *J. Am. Chem. Soc.*, 2005, **127**, 15040–15041.

63 T. Caruso, A. Capobianco and A. Peluso, *J. Am. Chem. Soc.*, 2007, **129**, 15347–15353.

64 A. Capobianco, M. Carotenuto, T. Caruso and A. Peluso, *Angew. Chem. Int. Ed.*, 2009, **48**, 9526–9528.

65 X. Yang, X.-B. Wang, E. R. Vorpagel and L.-S. Wang, *Proc. Natl. Acad. Sci. USA*, 2004, **101**, 17588–17592.

66 O. I. Kovalsky, I. G. Panyutin and E. I. Budowsky, *Photochem. Photobiol.*, 1990, **52**, 509–517.

67 I. Saito, M. Takayama, H. Sugiyama, K. Nakatani, A. Tsuchida and M. Yamamoto, *J. Am. Chem. Soc.*, 1995, **117**, 6406–6407.

68 H. Sugiyama and I. Saito, *J. Am. Chem. Soc.*, 1996, **118**, 7063–7068.

69 J. G. Muller, R. P. Hickerson, R. J. Perez and C. J. Burrows, *J. Am. Chem. Soc.*, 1997, **119**, 1501–1506.

70 K. Nakatani, K. Fujisawa, C. Dohno, T. Nakamura and I. Saito, *Tetrahedron Lett.*, 1998, **39**, 5995–5998.

71 Y. Yoshioka, Y. Kitagawa, Y. Takano, K. Yamaguchi, T. Nakamura and I. Saito, *J. Am. Chem. Soc.*, 1999, **121**, 8712–8719.

72 R. P. Hickerson, F. Prat, J. G. Muller, C. S. Foote and C. J. Burrows, *J. Am. Chem. Soc.*, 1999, **121**, 9423–9428.

73 K. Nakatani, C. Dohno and I. Saito, *J. Am. Chem. Soc.*, 2000, **122**, 5893–5894.

74 M. S. Cooke, M. D. Evans, M. Dizdaroglu and J. Lunec, *FASEB J.*, 2003, **17**, 1195–1214.

75 J. Abraham, A. K. Gosh and G. B. Schuster, *J. Am. Chem. Soc.*, 2006, **128**, 5346–5347.

76 M. Bixon, B. Giese, S. Wessely, T. Langenbacher, M. E. Michel-Beyerle and J. Jortner, *Proc. Natl. Acad. Sci. USA*, 1999, **96**, 11713–11716.

77 T. Renger and R. A. Marcus, *J. Phys. Chem. A*, 2003, **107**, 8404–8419.

78 A. Troisi and G. Orlandi, *Chem. Phys. Lett.*, 2001, **344**, 509–518.

79 A. Troisi and G. Orlandi, *J. Phys. Chem. B*, 2002, **106**, 2093–2101.

80 S. Kanvah, J. Joseph, G. B. Schuster, R. N. Barnett, C. L. Cleveland and U. Landman, *Acc. Chem. Res.*, 2010, **43**, 280–287.

81 K. Kawai and T. Majima, *Acc. Chem. Res.*, 2013, **46**, 2616–2625.

82 F. D. Lewis, H. Zhu, P. Daublain, T. Fiebig, M. Raytchev, Q. Wang and V. Shafirovich, *J. Am. Chem. Soc.*, 2006, **128**, 791–800.

83 K. Kawai and T. Majima, *Acc. Chem. Res.*, 2013, **46**, 2616–2625.

84 A. K. Thazhathveetil, A. Trifonov, M. R. Wasielewski and F. D. Lewis, *J. Am. Chem. Soc.*, 2011, **133**, 11485–11487.

85 K. Kawai, H. Kodera, Y. Osakada and T. Majima, *Nat. Chem.*, 2009, **1**, 156–159.

86 J. Vura-Weis, M. R. Wasielewski, A. K. Thazhathveetil and F. D. Lewis, *J. Am. Chem. Soc.*, 2009, **131**, 9722–9727.

87 N. Reanaud, Y. A. Berlin, F. D. Lewis and M. A. Ratner, *J. Am. Chem. Soc.*, 2013, **135**, 3953–3963.

88 A. Capobianco, T. Caruso, M. Celentano, A. M. D'Ursi, M. Scrima and A. Peluso, *J. Phys. Chem. B*, 2013, **117**, 8947–8953.

89 A. Capobianco and A. Peluso, *RSC Adv.*, 2014, **4**, 47887–47893.

90 A. Capobianco, T. Caruso and A. Peluso, *Phys. Chem. Chem. Phys.*,

2015, **17**, 4750– 4756.

91  J. Jortner, M. Bixon, T. Langenbacher and M. E. Michel-Beyerle, *Proc. Natl. Acad. Sci. USA*, 1998, **95**, 12759.

92  A. Voityuk, J. Jortner, M. Bixon and N. Rösch, *Chem. Phys. Lett.*, 2000, **324**, 430–434.

93  A. Voityuk, J. Jortner, M. Bixon and N. Rösch, *J. Chem. Phys.*, 2001, **114**, 5614–5620.

94  K. Senthilkumar, F. C. Grozema, C. F. Guerra, F. M. Bickelhaupt and L. D. A. Siebbeles, *J. Am. Chem. Soc.*, 2003, **125**, 13658–13659.

95  K. Senthilkumar, F. C. Grozema, C. F. Guerra, F. M. Bickelhaupt, F. D. Lewis, Y. A. Berlin, M. A. Ratner and L. D. A. Siebbeles, *J. Am. Chem. Soc.*, 2005, **127**, 14894–14903.

96  F. C. Grozema, S. Tonzani, Y. A. Berlin, G. C. Schatz, L. D. A. Siebbeles and M. A. Ratner, *J. Am. Chem. Soc.*, 2008, **130**, 5157–5166.

97  F. C. Grozema, S. Tonzani, Y. A. Berlin, G. C. Schatz, L. D. A. Siebbeles and M. A. Ratner, *J. Am. Chem. Soc.*, 2009, **131**, 14204–14205.

98  Y. A. Berlin, I. V. Kurnikov, D. Beratan, M. A. Ratner and A. L. Burin, *Long-Range Charge Transfer in DNA II*, Springer Berlin Heidelberg, 2004, vol. 237, pp. 1–36.

99  R. Borrelli, A. Capobianco and A. Peluso, *Chem. Phys.*, 2014, **440**, 25–30.

100  B. Giese, J. Amaudrut, A.-K. Köhler, M. Spormann and S. Wessely, *Nature*, 2001, **412**, 318–320.

101  R. Borrelli, A. Capobianco and A. Peluso, *Chem. Phys.*, 2014, **440**, 25–30.

102  R. Borrelli and W. Domcke, *Chem. Phys. Lett.*, 2010, **498**, 230.

103  R. Borrelli, M. Thoss, H. Wang and W. Domcke, *Mol. Phys.*, 2012, **110**, 751.

104  R. Borrelli and A. Peluso, *WIREs: Comput. Mol. Sci.*, 2013, **3**, 542–559.

105  A. Capobianco, T. Caruso, M. Celentano, M. V. La Rocca and A. Peluso, *J. Chem. Phys.*, 2013, **139**, 145101.

106  F. D. Lewis, X. Liu, J. Liu, R. T. Hayes and M. R. Wasielewski, *J. Am. Chem. Soc.*, 2000, **122**, 12037–12038.

107  L. V. Kurnikov, G. S. M. Tong, M. Madrid and D. N. Beratan, *J. Phys. Chem. B*, 2002, **106**, 7–10.

108  D. M. Basko and E. M. Conwell, *Phys. Rev. Lett.*, 2002, **88**, 098102.

109  K. E. Augustyn, J. C. Genereux and J. K. Barton, *Angew. Chem. Int. Ed.*, 2007, **46**, 5731–5733.

110  J. Tomasi, B. Mennucci and R. Cammi, *Chem. Rev.*, 2005, **105**, 2999–3094.

111  M. J. Frisch, G. W. Trucks, H. B. Schlegel, G. E. Scuseria, M. A. Robb, J. R. Cheeseman, G. Scalmani, V. Barone, B. Mennucci, G. A. Peterson, H. Nakatsuji, M. Caricato, X. Li, H. P. Hratchian, A. F. Izmaylov, J. Bloino, G. Zheng, J. L. Sonnenberg, M. Hada, M. Ehara, K. Toyota, R. Fukuda, J. Hasegawa, M. Ishida, T. Nakajima, Y. Honda, O. Kitao, H. Nakai, T. Vreven, J. A. Montgomery, Jr., J. E. Peralta, F. Ogliaro, M. Bearpark, J. J. Heyd, E. Brothers, K. N. Kudin, V. N. Staroverov, R. Kobayashi, J. Normand, K. Raghavachari, A. Rendell, J. C. Burant, S. S. Iyengar, J. Tomasi, M. Cossi, N. Rega, J. M. Millam, M. Klene, J. E. Knox, J. B. Cross, V. Bakken, C. Adamo, J. Jaramillo, R. Gomperts, R. E. Stratmann, O. Yazyev, A. J. Austin, R. Cammi, C. Pomelli, J. W. Ochterski, R. L. Martin, K. Morokuma, V. G. Zakrzewski, G. A. Voth, P. Salvador, J. J. Dannenberg, S. Dapprich, A. D. Daniels, Ö. Farkas, J. B. Foresman, J. V. Ortiz, J. Cioslowski and D. J. Fox, *Gaussian 09 Revision D.01*, Gaussian Inc. Wallingford CT 2009.

112  R. Borrelli and A. Peluso, *MolFC: A program for Franck-Condon integrals calculation*, Package available online at http://www.theochem.unisa.it.

113  R. Borrelli, A. Capobianco and A. Peluso, *Can. J. Chem.*, 2013, **91**, 495–504.

114  R. Borrelli, A. Capobianco and A. Peluso, *J. Phys. Chem. A*, 2012, **116**, 9934.

115  R. Borrelli and A. Peluso, *J. Chem. Phys.*, 2013, **139**, 159902.

116  A. Peluso, R. Borrelli and A. Capobianco, *J. Phys. Chem. A*, 2009, **113**, 14831.

117  A. Peluso, R. Borrelli and A. Capobianco, *J. Phys. Chem. A*, 2013, **117**, 10985–10985.

118  A. Capobianco, R. Borrelli, C. Noce and A. Peluso, *Theor. Chem. Acc.*, 2012, **131**, 1181.

119  J. T. Park and J. C. Light, *J. Chem. Phys.*, 1986, **85**, 5870–5876.